ν-Nucleus interaction in the Spectral Function formalism

Noemi Rocco, O. Benhar, A. Lovato

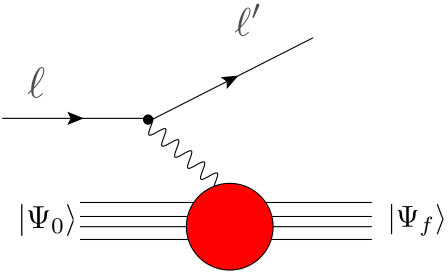

"Lepton-Nucleus Scattering XIV Workshop"

Marciana Marina, Isola d'Elba
June 27-July 1, 2016

- Based on: O.Benhar, A.Lovato, and NR, Phys. Rev. C **92**, 024602 (2015);
- NR, A.Lovato, and O.Benhar, PRL **116**, 192501 (2016).

Outline

- Motivations
  - Accurate determination of neutrino oscillation parameter
  - Differences between electron- and neutrino- nucleus scattering
- Non relativistic & relativistic regimes: the factorization scheme.
- Meson-exchange currents in the extended factorization ansatz
- Comparison to experimental data
- Summary & Outlook

Motivations

- Studying neutrino properties is one of the most exciting challenges of particle physics. The extreme complexity of this task is due to the eminently elusive nature of these particles. In Leon Lederman's words:
  "Neutrinos ... win the minimalist contest: zero charge, zero radius, and very possibly zero mass."
- Precise measurements of the oscillation parameters involves the analysis of the neutrino interactions with a target nucleus.
- Accurate theoretical models of electron- nucleus scattering provide a satisfactory description of the experimental data.

Motivations

- Studying neutrino properties is one of the most exciting challenges of particle physics. The extreme complexity of this task is due to the eminently elusive nature of these particles. In Leon Lederman's words: ''Neutrinos ... win the minimalist contest: zero charge, zero radius, and very possibly zero mass.''
- Precise measurements of the oscillation parameters involves the analysis of the neutrino interactions with a target nucleus.
- Accurate theoretical models of electron- nucleus scattering provide a satisfactory description of the experimental data.

Motivations

- Studying neutrino properties is one of the most exciting challenges of particle physics. The extreme complexity of this task is due to the eminently elusive nature of these particles. In Leon Lederman's words:
  <u>"Neutrinos ... win the minimalist contest: zero charge, zero radius, and very possibly zero mass."</u>
- Precise measurements of the oscillation parameters involves the analysis of the neutrino interactions with a target nucleus.
- Accurate theoretical models of electron- nucleus scattering provide a satisfactory description of the experimental data.

QE electron- & neutrino-nucleus cross sections

- Data: MiniBooNE Collaboration
- Data: J.S. O'Connell *et al*

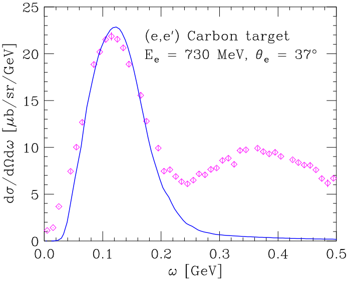

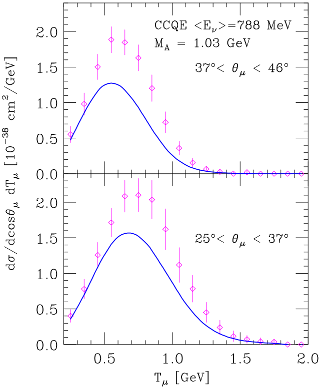

- The calculations performed using the spectral function and the measured nuclear vector form factors accurately reproduce the QE peak measured in electron scattering
- The same scheme largely fails to explain the MiniBooNE data.

The axial mass puzzle

- Unfolded total CCQE cross section

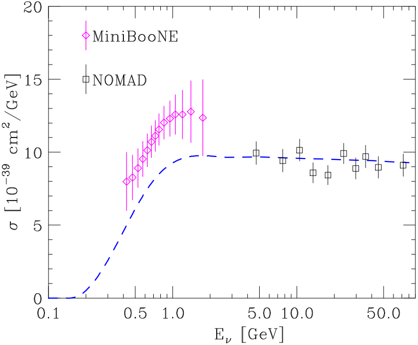

- The axial form factor is generally parametrized in the dipole form

$$F_A(Q^2) = \frac{g_A}{\left[1 + (Q^2/M_A^2)\right]^2} ,$$

- Deuteron data $\Rightarrow$ $M_A \approx 1.03$ GeV
- MiniBooNE $\Rightarrow$ $M_A \approx 1.35$ GeV
- K2K $\Rightarrow$ $M_A \approx 1.2$ GeV
- NOMAD $\Rightarrow$ $M_A \approx 1.05$ GeV

- Interpret the value of M_A reported by MiniBooNE as an *effective* axial mass, modified by nuclear effects not included in the RFGM.

Role of Multi Nucleon knockout

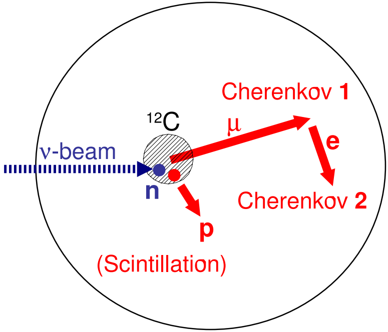

- In MiniBooNE data analysis an event is labeled as CCQE if no final state pions are detected in addition to the outgoing muon.
- The simplest reaction mechanism compatible with this definition is single nucleon knockout

The observed excess of CCQE cross-section may be traced back to the occurrence of events with two particle-two hole final states, which are often referred to CCQE-like.

Inclusive lepton-nucleus cross section at fixed beam energy

Inclusive electron-nucleus cross section at $E_e \sim 1$ GeV, as a function of ω.

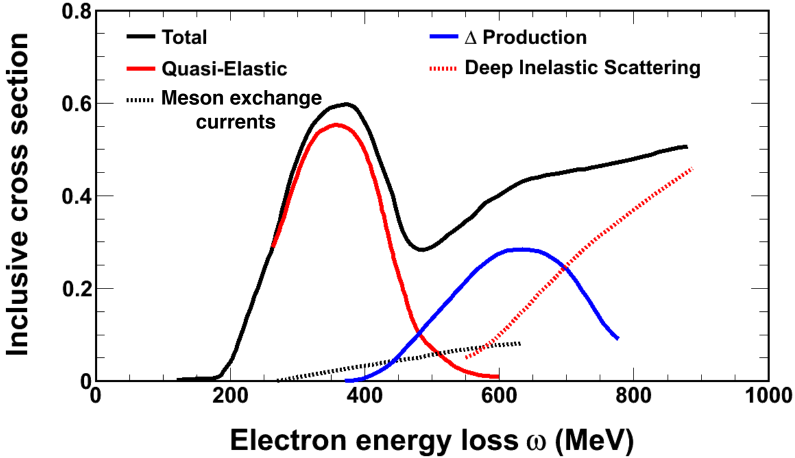

The different reaction mechanisms, contributing to the cross section at different values of ω, can be easily identified.

QE neutrino-nucleus scattering

- The measured double differential CCQE cross section is averaged over the neutrino flux

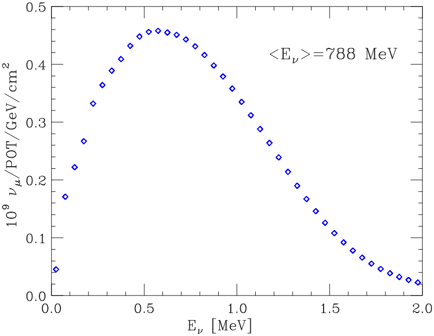

- Energy distribution of MiniBooNE neutrino flux
- Different reaction mechanisms contribute to the cross section at fixed θ_μ and T_μ.

A description of neutrino-nucleus interactions, has to be validated through extensive comparison to the large body of electron-nucleus scattering data.

The electron-nucleus x-section

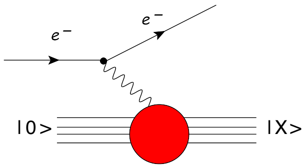

- The double differential x-section of the process $e^- + A \to e^- + X$, can be written as

$$\frac{d^2\sigma}{d\Omega_{\mathbf{k}'} dk'_0} = \frac{\alpha^2}{Q^4} \frac{E'_e}{E_e} L_{\mu\nu} W_A^{\mu\nu} \ .$$

- $L_{\mu\nu}$ is completely determined by the lepton kinematics
- The hadronic tensor describes the response of the target nucleus.

$$W_A^{\mu\nu} = \sum_X \langle 0|J_A^{\mu\dagger}|X\rangle \langle X|J_A^{\nu}|0\rangle \ \delta^{(4)}(p_0 + q - p_X) \ ,$$

initial state

$|0\rangle$; p_0

final state

$|X\rangle = |1p;1h\rangle, |2p;2h\rangle \ldots$; p_X

Non relativistic nuclear many-body theory (NMBT) provides a fully consistent theoretical approach allowing for an accurate description of $|0\rangle$, independent on momentum transfer.

CCQE interactions at moderate ($|q| \lesssim 500$ MeV)

- Within NMBT the nucleus is described as a collection of A pointlike nucleons, the dynamics of which are described by the nonrelativistic Hamiltonian

$$H = \sum_{i=1}^{A} \frac{p_i^2}{2m} + \sum_{j>i=1}^{A} v_{ij} + \sum_{k>j>i=1}^{A} V_{ijk}$$

Argonne v18

UIX, IL7

- Initial state definition:

$$H|0\rangle = E_0|0\rangle$$

- Final state definition

$$H|X\rangle = E_X|X\rangle$$

The above Schrödinger equation can only be exactly solved for the ground- and low-lying excited states of nuclei with $A \leq 12$.

The nuclear current operator

- The nuclear Hamiltonian does not commute with the charge density operator: $[H, J^0] \neq 0$
- In order for the continuity equation to be satisfied two body currents are needed:

$$\frac{\partial}{\partial t} J^0 + \vec{\nabla} \cdot \vec{J} = 0$$

- The nuclear current includes one-and two-nucleon contributions

$$J_A^\mu(q) = \sum_{i=1}^{A} j_i^\mu(q) + \sum_{j>i=1}^{A} j_{ij}^\mu(q_1, q_2)\delta(q - q_1 - q_2)$$

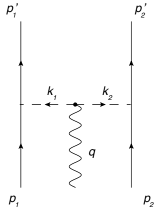

- non relativistic reduction of the current (q/m expansions) .

Kinematical range of accelerator-based neutrino experiments

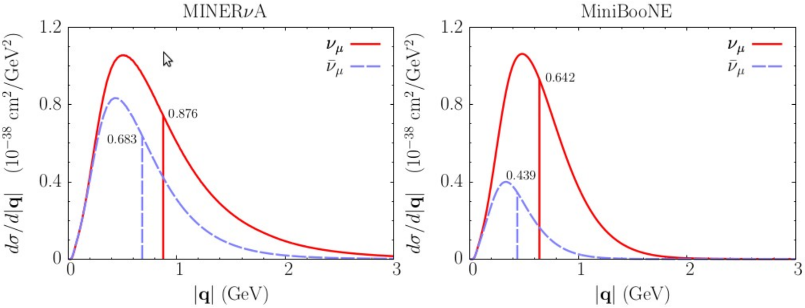

- $|q|$-dependence of CCQE cross section averaged with the Minerνa and MiniBooNE fluxes

WARNING!

unlike the ground state, the nuclear current operator and the nuclear final state depend on momentum transfer. At large **q** non relativistic approximations become inadequate.

The *factorization "paradigm"*

- Simplest implementation: Impulse Approximation (IA)

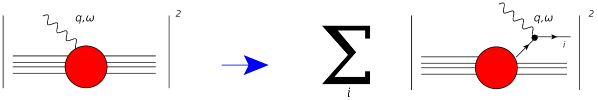

- At $|\mathbf{q}|^{-1} \ll d$:

$$J_A^\mu \longrightarrow \sum_i j_i^\mu \ , \qquad |X\rangle \longrightarrow |x, \mathbf{p}_x\rangle \otimes |R, \mathbf{p}_R\rangle \ ,$$

- The nuclear cross section can be traced back to the one describing the interaction with individual bound nucleons

$$d\sigma_A = \int dEd^3k \ d\sigma_N \ P(k, E)$$

  - An integration on the nucleon momentum and removal energy is carried out, with a weight given by the **Spectral Function**

The impact of relativistic effects

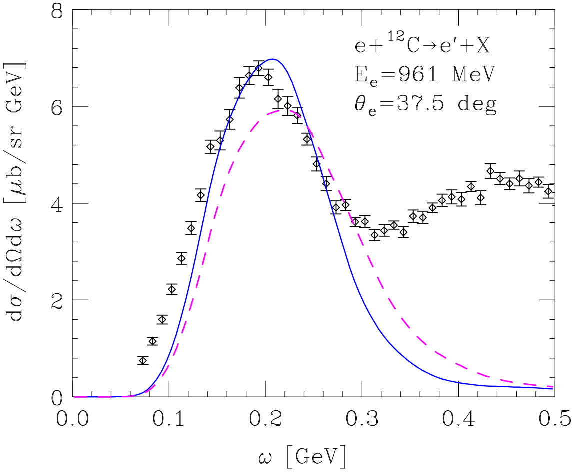

Electron-carbon cross section obtained within the IA approach using relativistic (solid line) and non relativistic (dashed line) kinematics.

- In a kinematical setup corresponding to $|q| \sim 585$ MeV at $\omega = \omega_{QE}$ relativistic kinematics sizeably affects both position and width of the quasi elastic peak.

Spectral function and energy-momentum distribution

- Oxygen spectral function, obtained within LDA.

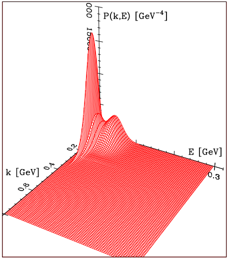

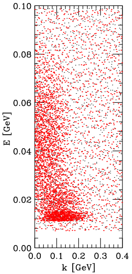

$$P_{LDA}(\mathbf{p},E) = \boxed{P_{MF}(\mathbf{p},E)} + \boxed{P_{\rm corr}(\mathbf{p},E)}$$

$$\sum_{n\in\{F\}} Z_n|\phi_n(\mathbf{p})|^2 F_n(E-E_n) \qquad \int d^3r\,\varrho_A(\mathbf{r})P^{NM}_{\rm corr}(\mathbf{p},E;\varrho=\varrho_A(\mathbf{r}))$$

- Momentum and removal energy sampled from LDA (red) and RFGM (green) oxygen spectral functions

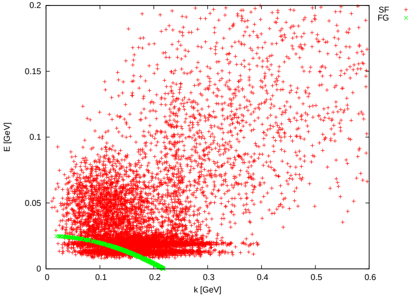

- Scattering off high momentum and high removal energy nucleons, providing ~ 20 % of the total strength.

Range of applicability of the IA

- Electron-Carbon cross section for $E_e = 1.3$ GeV, $\theta_e = 37.5$.

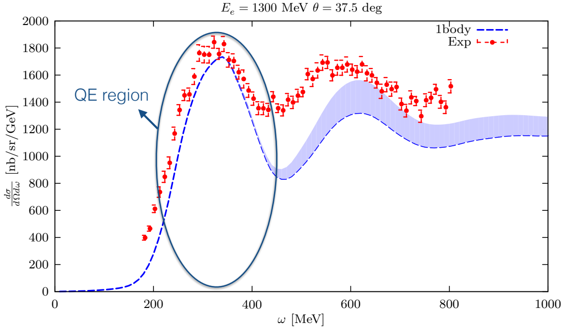

$$\widetilde{w}_1^N = \tau \; G_{MN}^2 \; \delta\Big(\tilde{\omega} + \frac{\tilde{q}^2}{2m}\Big),$$

$$\widetilde{w}_2^N = \frac{1}{(1+\tau)}\Big(G_{EN}^2 + \tau G_{MN}^2\Big) \; \delta\Big(\tilde{\omega} + \frac{\tilde{q}^2}{2m}\Big)$$

Range of applicability of the IA

- Electron-Carbon cross section for $E_e = 1.3$ GeV, $\theta_e = 37.5$.

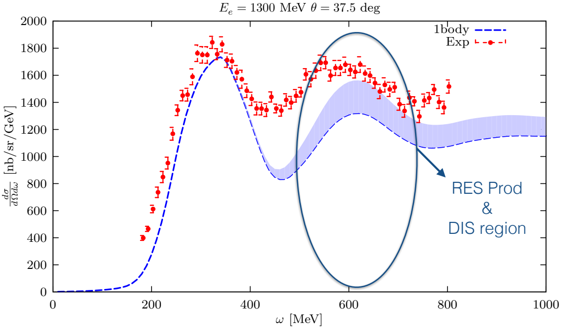

The inelastic nucleon structure functions are extracted from the analysis of electron-proton and electron-deuteron scattering data (Bodek-Ritchie).

- Electron-Carbon cross section for $E_e = 1.3$ GeV, $\theta_e = 37.5$.

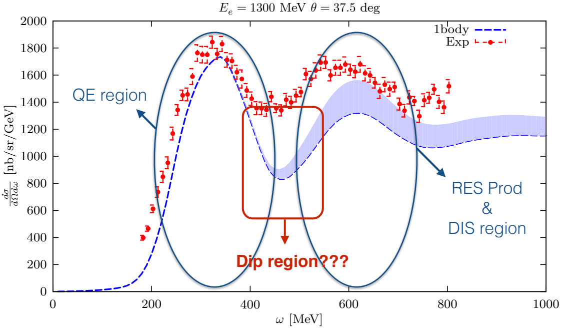

- The contribution of two-body currents has to be included. These are expected to play a significant role in the so called *dip region*.

Role of reaction mechanism beyond IA

- Scaling functions associated with the longitudinal (L) and transverse (T) response of Carbon extracted from electron scattering data

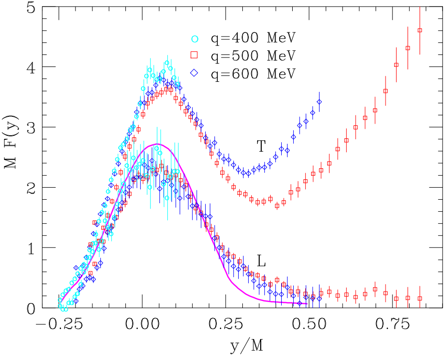

  - the onset of scaling is clearly visible in the region of QE peak, corresponding to $y \sim 0$.
  - large scaling violations appear in $F_T(y)$ at $y > 0$.

Role of reaction mechanism beyond IA

J.Carlson, J. Jourdan, R. Schiavilla, and I. Sick, Phys. Rev. C 65, 024002 (2002)

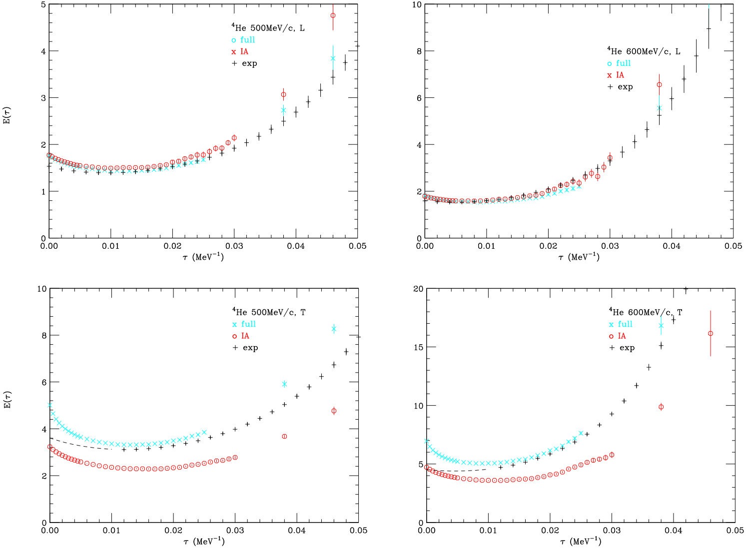

How can 2p2h final states be produced?

In a model accounting for NN correlations, 2p2h final states can be produced through 3 different reaction mechanisms.

- Initial State Correlations (ISC):

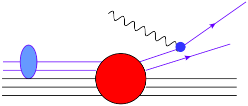

- Meson Exchange Currents (MEC):

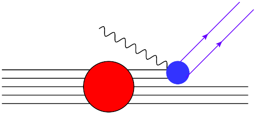

- Final State Interactions (FSI):

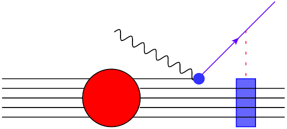

(a)

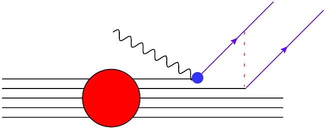

(b)

Extending the factorization scheme

- Using relativistic MEC and a realistic description of the nuclear ground state requires the extension of the factorization scheme to two-nucleon emission amplitude

  - Rewrite the hadronic final state $|X\rangle$ in the factorized form:

$$|X\rangle \longrightarrow |\mathbf{p}\ \mathbf{p}'\rangle \otimes |n_{(A-2)}\rangle = |n_{(A-2)}; \mathbf{p}\ \mathbf{p}'\rangle \ ,$$

    where $|n_{(A-2)}\rangle$ describes the spectator $(A-2)$-nucleon system, carrying momentum $\mathbf{p}_n$.

  - The two nucleon current simplifies

$$\langle X|{j_{ij}}^{\mu}|0\rangle \rightarrow \int d^3k d^3k' M_n(\mathbf{k},\mathbf{k}') \ \langle \mathbf{p}\mathbf{p}'|{j_{ij}}^{\mu}|\mathbf{k}\mathbf{k}'\rangle \ \delta(\mathbf{k}+\mathbf{k}'-\mathbf{p}_n) \ ,$$

  - The nuclear amplitude: $M_n(\mathbf{k},\mathbf{k}') = \langle n_{(A-2)}; \mathbf{k}\ \mathbf{k}'|0\rangle$
    is independent of $\mathbf{q}$, and can therefore be obtained within NMBT.

Two nucleon spectral function

- Two-nucleon spectral function of uniform and isospin nuclear matter

$$P(\mathbf{k},\mathbf{k}',E) = \sum_n |M_n(\mathbf{k},\mathbf{k}')|^2 \delta(E + E_0 - E_n)$$

$$n(\mathbf{k},\mathbf{k}') = \int dE \; P(\mathbf{k},\mathbf{k}',E)$$

- Relative momentum distribution

$$n(\mathbf{Q}) = 4\pi|\mathbf{Q}|^2 \int d^3K\, n\left(\mathbf{Q}+\frac{\mathbf{K}}{2},\mathbf{Q}-\frac{\mathbf{K}}{2}\right)$$

$$\mathbf{K} = \mathbf{k}+\mathbf{k}' \quad , \quad \mathbf{Q} = \frac{\mathbf{k}-\mathbf{k}'}{2} \; .$$

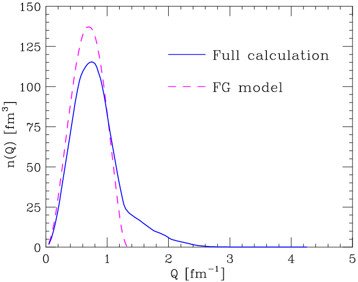

  - Correlation effects lead to a quenching of the peak of the distributions and an enhancement of the high momentum tail

1p1h and 2p2h contributions to the nuclear cross section

- **The factorization scheme allows for a clear identification of the 1p1h and 2p2h contributions**

$$d\sigma = d\sigma_{\rm 1p1h} + d\sigma_{\rm 2p2h} \propto L_{\mu\nu}(W^{\mu\nu}_{\rm 1p1h} + W^{\mu\nu}_{\rm 2p2h})$$

- **2p2h response tensor**

$$W^{\mu\nu}_{2p2h} = \sum_{h,h'<k_F} \sum_{p,p'>k_F} \langle 0|J^{\mu\,\dagger}|\mathbf{hh'pp'}\rangle\langle \mathbf{hh'pp'}|J^\nu|0\rangle \times \delta(\omega + E_0 - E_{hh'pp'})\delta(\mathbf{q}+\mathbf{h}+\mathbf{h}'-\mathbf{p}-\mathbf{p}') \ ,$$

- **Current operator in momentum space:**

$$J^\mu(\mathbf{k_1},\mathbf{k_2}) = j_1^\mu(\mathbf{k_1})\delta(\mathbf{k_2}) + j_2^\mu(\mathbf{k_2})\delta(\mathbf{k_1}) + j_{12}^\mu(\mathbf{k_1},\mathbf{k_2}) \ ,$$

$$W^{\mu\nu}_{2p2h} = W^{\mu\nu}_{2p2h,11} + W^{\mu\nu}_{2p2h,22} + W^{\mu\nu}_{2p2h,12}$$

Production of 2p2h final states

1. **Initial state correlations**
2. MEC, two-body response
3. Interference

Initial state correlations

Within the IA...

$$W^{\mu\nu}_{2p2h,11} = \int d^3k \int dE\ P_{2h1p}(\mathbf{k}, E) w^{\mu\nu}_{11}$$

$$P_{2h1p}(\mathbf{k}, E) = \sum_{h,h' < k_F} \sum_{p' > k_F} |\Phi^{hh'p'}_k|^2$$
$$\times\ \delta(E + e_h + e_{h'} - e_{p'})\ ,$$

- appearence of the tail of the cross section, extending to large energy loss. This contribution amounts to $\sim$ 10% of the integrated spectrum.

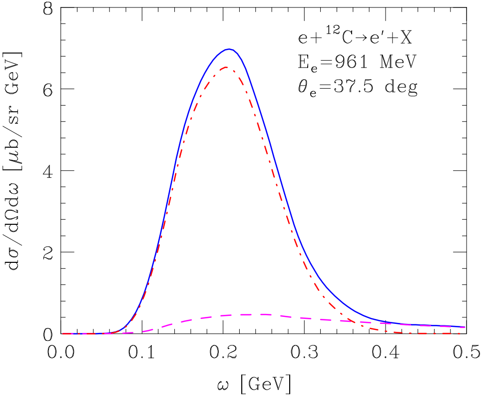

Production of 2p2h final states

1. Initial state correlations
2. MEC, two-body response
3. Interference

MEC: Pion exchange

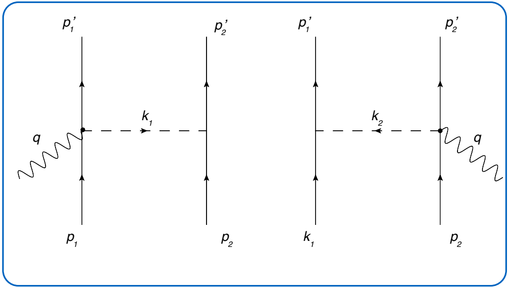

Seagull or contact term

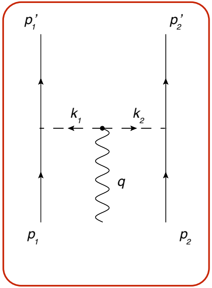

Pion in flight term

MEC: Δ-isobar exchange

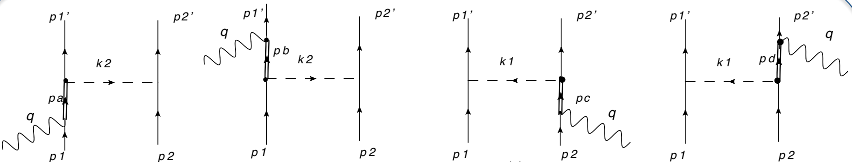

The Rarita-Schwinger (RS) expression for the Δ propagator reads

$$S^{\beta\gamma}(p, M_\Delta) = \frac{\not{p} + M_\Delta}{p^2 - M_\Delta^2}\left(g^{\beta\gamma} - \frac{\gamma^\beta\gamma^\gamma}{3} - \frac{2p^\beta p^\gamma}{3M_\Delta^2} - \frac{\gamma^\beta p^\gamma - \gamma^\gamma p^\beta}{3M_\Delta}\right)$$

WARNING

If the condition $p_\Delta^2 > (m_N + m_\pi)^2$ the real resonance mass has to be replaced by $M_\Delta \longrightarrow M_\Delta - i\Gamma(s)/2$ where $\Gamma(s) = \frac{(4f_{\pi N\Delta})^2}{12\pi m_\pi^2}\frac{k^3}{\sqrt{s}}(m_N + E_k)$.

2p-2h Transverse Response of nuclear matter

From the 2p-2h hadron tensor...

$$W^{\mu\nu}_{2p2h,22} = \int d^3k d^3k' d^3p d^3p' \int dE \; P_{2h}(\mathbf{k},\mathbf{k}',E) \langle \mathbf{k}\mathbf{k}'|j^{\mu}_{12}|\mathbf{p}\mathbf{p}'\rangle \langle \mathbf{p}\mathbf{p}'|j^{\nu}_{12}|\mathbf{k}\mathbf{k}'\rangle$$
$$\times \, \delta(\mathbf{k}+\mathbf{k}'+\mathbf{q}-\mathbf{p}-\mathbf{p}')\delta(\omega - E - e_p - e_{p'})\theta(|\mathbf{p}|-k_F)\theta(|\mathbf{p}'|-k_F) \; .$$

$$P_{2h}(\mathbf{k},\mathbf{k}',E) = \sum_{h,h'<k_F} |\Phi^{hh'}_{kk'}|^2 \delta(E + e_h + e_{h'})$$

- 12D integral, can be analitically reduced to a 7D integral $\rightarrow$ Monte Carlo integration technique
- both the direct and Pauli exchange contribution have to be considered (more than 100,000 terms) $\rightarrow$ Mathemathica and Fortran code

2p-2h Transverse Response of ^{12}C

Set of Harmonic Oscillator wave functions

$$\Psi_{0,0,0}(r) \Leftrightarrow \alpha = 1$$
$$\Psi_{0,1,1}(r) \Leftrightarrow \alpha = 2$$
$$\Psi_{0,1,-1}(r) \Leftrightarrow \alpha = 3$$

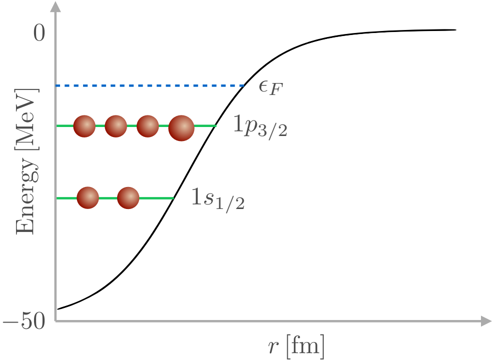

$$P_{2h}(\mathbf{k}, \mathbf{k}', E) = \sum_{\alpha_1,\alpha_2=1}^{3} Z_{\alpha_1} Z_{\alpha_2} |\Psi_{\alpha_1}(k)|^2 ||\Psi_{\alpha_2}(k')|^2 F(E + e_{\alpha_1}(k) + e_{\alpha_2}(k'))$$

$$e_1 = -38 MeV \ , \ e_{2,3} = -17.0 MeV \qquad Z_1 = 0.5 \ , \ Z_{2,3} = 0.625$$

Contribution of the MEC to the transverse response

Separate contributions to the transverse response function $R_T(\omega, q)$ at $q = 570$ MeV: pionic, pionic- Δ interference, Δ and total.

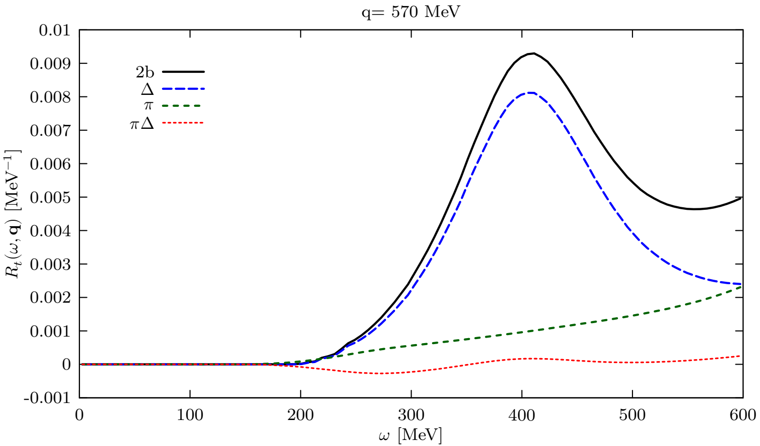

Beyond the RFGM ...

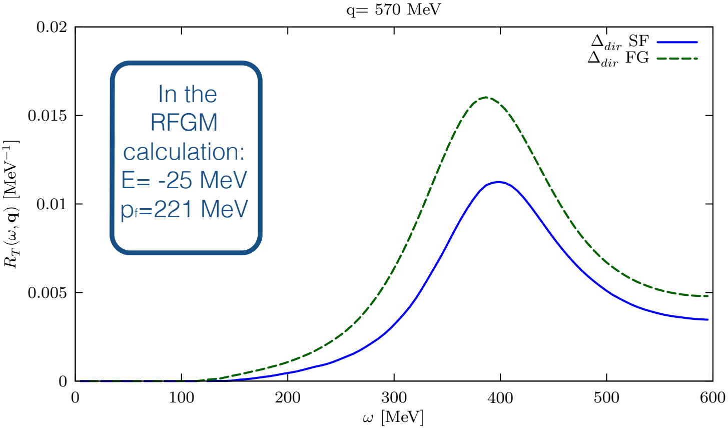

Sizable differences

Different threshold $\Rightarrow$ different treatment of the initial state energies of the knocked-out nucleons.

Significant quenching of the response $\Rightarrow$ short range correlations.

Non Relativistic expression of the 2p2h contribution to $R_T(\omega, q)$

PHYSICAL REVIEW C VOLUME 49, NUMBER 5 MAY 1994

Relativistic meson exchange and isobar currents in electron scattering: Noninteracting Fermi gas analysis

M. J. Dekker* and P. J. Brussaard
R. J. Van de Graaff Laboratory, University of Utrecht, P.O Box 80.000, 3508 TA Utrecht, The Netherlands

J. A. Tjon
Institute for Theoretical Physics, University of Utrecht, P.O Box 80.000, 3508 TA Utrecht, The Netherlands
(Received 22 November 1993)

$$
\begin{aligned}
\mathcal{R}_T = {} & 64c_N^2\left[2\frac{\mathbf{k}_1^2}{(\mathbf{k}_1^2+m_\pi^2)^2}+\mathbf{k}_{1_T}^2\left(2\frac{\mathbf{k}_1^2\mathbf{k}_2^2}{(\mathbf{k}_1^2+m_\pi^2)^2(\mathbf{k}_2^2+m_\pi^2)^2}-4\frac{\mathbf{k}_1^2}{(\mathbf{k}_1^2+m_\pi^2)^2(\mathbf{k}_2^2+m_\pi^2)}+\frac{1}{(\mathbf{k}_1^2+m_\pi^2)(\mathbf{k}_2^2+m_\pi^2)}\right)\right] \\
& +64c_\Delta^2\mathbf{k}_1^2\left(\mathbf{k}_1^2\mathbf{q}^2(2\tilde{b}^2+\tilde{a}^2)-(2\tilde{b}^2-\tilde{a}^2)(\mathbf{k}_1\cdot\mathbf{q})^2\right)\frac{1}{(\mathbf{k}_1^2+m_\pi^2)^2}+64c_\Delta^2\,\tilde{a}^2\frac{\mathbf{q}^4\mathbf{k}_{1_T}^2}{(\mathbf{k}_1^2+m_\pi^2)(\mathbf{k}_2^2+m_\pi^2)} \\
& +64c_\Delta c_{\mathrm{N}}\,\tilde{a}\left(\frac{4\mathbf{q}^2\mathbf{k}_1^2\mathbf{k}_{1_T}^2}{(\mathbf{k}_1^2+m_\pi^2)^2(\mathbf{k}_2^2+m_\pi^2)}-2\frac{\mathbf{q}^2\mathbf{k}_{1_T}^2}{(\mathbf{k}_1^2+m_\pi^2)(\mathbf{k}_2^2+m_\pi^2)}-4\frac{\mathbf{k}_1^2\mathbf{k}_1\cdot\mathbf{q}}{(\mathbf{k}_1^2+m_\pi^2)^2}\right)+(1\leftrightarrow 2)
\end{aligned}
\tag{5.11}
$$

Relativity dramatically affects the behaviour of the response.

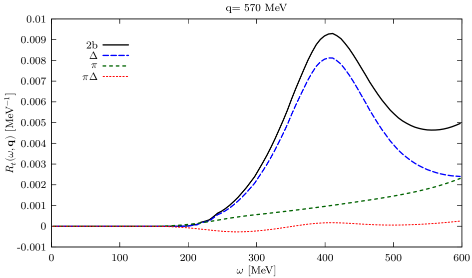

Relativistic

Nonrelativistic

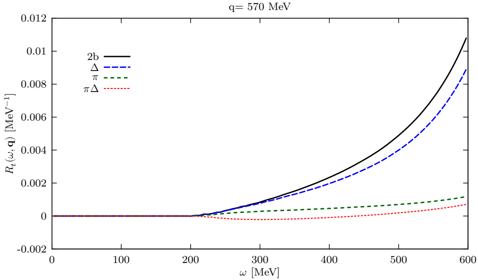

The impact of relativistic effects in the two-body response

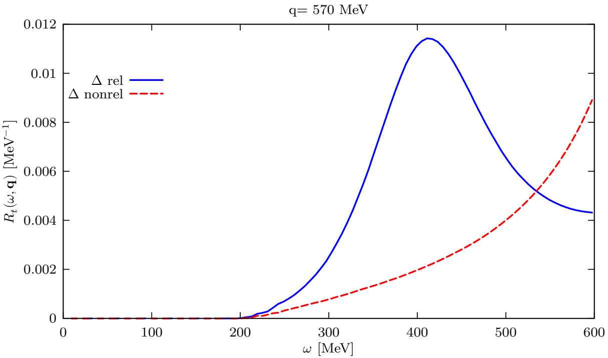

The most important effect introduced by relativity is the peak produced by the dynamic Δ-propagation.

The overall effects are small in the domain of the QEP, modest in the dip region and substantial in the region of the Δ-peak. Beyond the Δ peak, relativity yields a substantial reduction of the response.

Production of 2p2h final states

1. Initial state correlations
2. MEC, two-body response
3. **Interference**

Interference term

It cannot be written in terms of SF...

$$W^{\mu\nu}{}_{2p2h,12} = \int d^3k \; d^3\xi \; d^3\xi' \; d^3h \; d^3h' d^3p \; d^3p' \phi^{hh'\,*}_{\xi\xi'} \Big[\Phi^{hh'p'}_{k} \langle \mathbf{k} | j^{\mu}_{1} | \mathbf{p} \rangle + \Phi^{hh'p}_{k} \langle \mathbf{k} | j^{\mu}_{2} | \mathbf{p}' \rangle \Big] \langle \mathbf{p}, \mathbf{p}' | j^{\nu}_{12} | \boldsymbol{\xi}, \boldsymbol{\xi}' \rangle \delta(\mathbf{h} + \mathbf{h}' + \mathbf{q} - \mathbf{p} - \mathbf{p}') \times \delta(\omega + e_h + e_{h'} - e_p - e_{p'}) \theta(|\mathbf{p}| - k_F) \theta(|\mathbf{p}'| - k_F) + \mathrm{h.c.}\;.$$

Additional difficulty... This term involves the product of nuclear amplitudes entering in $P(k, E)$ and $P(k, k', E)$

WARNING

This interference contribution would be zero if correlations were not accounted for!

^{12}C electromagnetic response

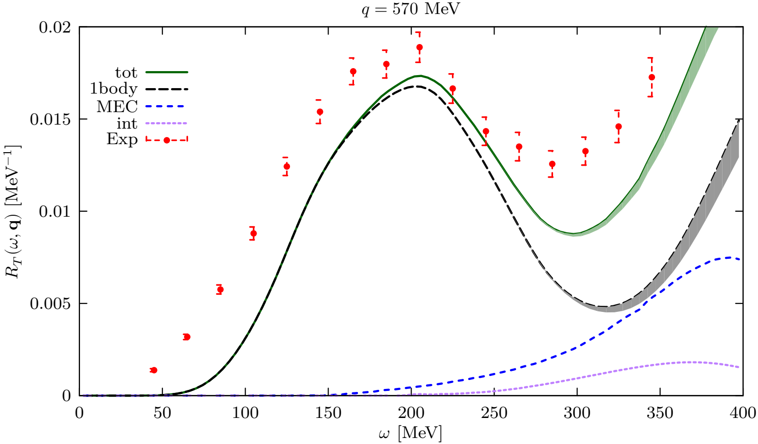

^{12}C calculations indicate a sizable enhancement of the electromagnetic transverse response.

Inclusion of Final State Interaction contribution

Convolution scheme

$$\frac{d\sigma^{\rm FSI}}{d\omega d\Omega} = \int d\omega' \; f_{\mathbf{q}}(\omega - \omega') \frac{d\sigma^{\rm IA}}{d\omega d\Omega}$$

The folding function can be decomposed in the form

$$f_{\mathbf{q}}(\omega) = \delta(\omega)\sqrt{T_A} + (1 - \sqrt{T_A})F_{\mathbf{q}}(\omega)$$

showing that the strength of FSI is driven by

- the nuclear transparency T_A
- the finite-width function $F_{\mathbf{q}}(\omega)$

- A.Ankowski *et al.*, Phys. Rev. D 91, 033005 (2015)
- O. Benhar, Phys. Rev. C 87, 024606 (2013).

e^- - ^{12}C inclusive cross section

The x-section can be rewritten in terms of R_T and R_L such as

$$\frac{d\sigma}{dE'_e d\Omega} = \sigma_{Mott}\left[\left(\frac{q^2}{\mathbf{q}^2}\right)^2 R_L + \left(\frac{-q^2}{2\mathbf{q}^2} + tan^2\frac{\theta}{2}\right) R_T\right]$$

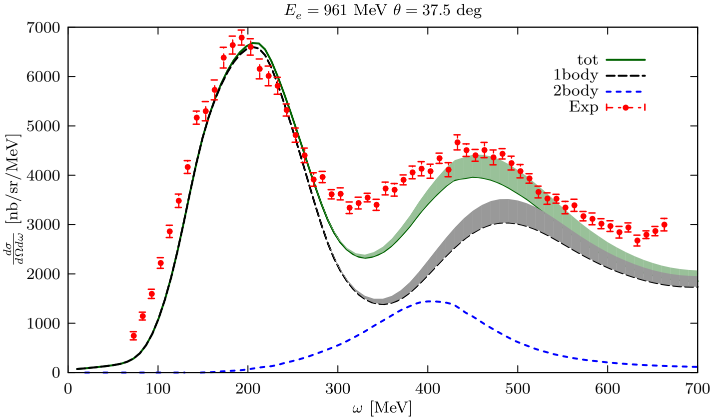

e^- - ^{12}C inclusive cross section

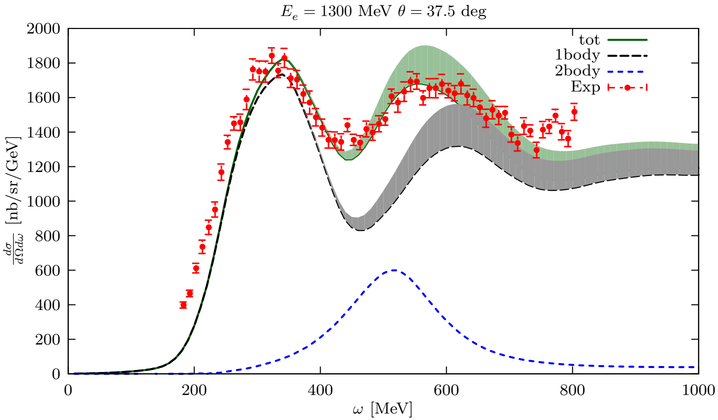

The contribution given by the interference term and MEC currents turns out to be sizable in the *dip* region.

e^{-} - ^{12}C inclusive cross section

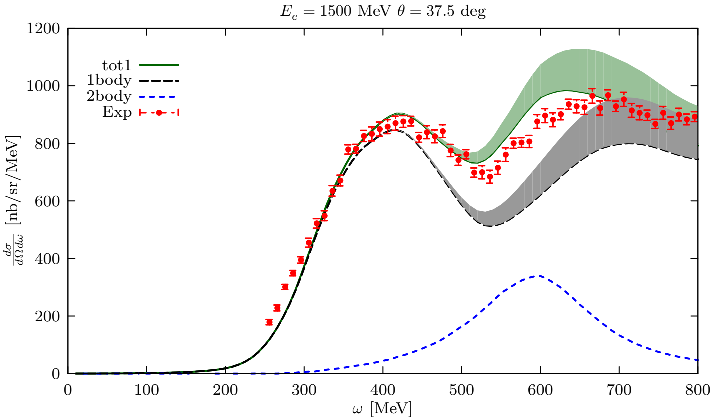

The contribution given by the interference term and MEC currents turns out to be sizable in the *dip* region.

May MEC explain the MiniBooNE data?

- It is apparent that the disagreement between theoretical calculations not including MEC and data is less pronounced at small θ_μ

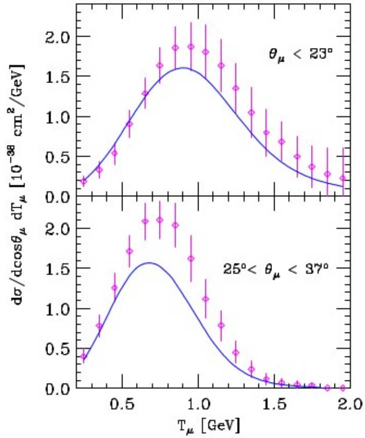

Angular dependence of the two-body contribution

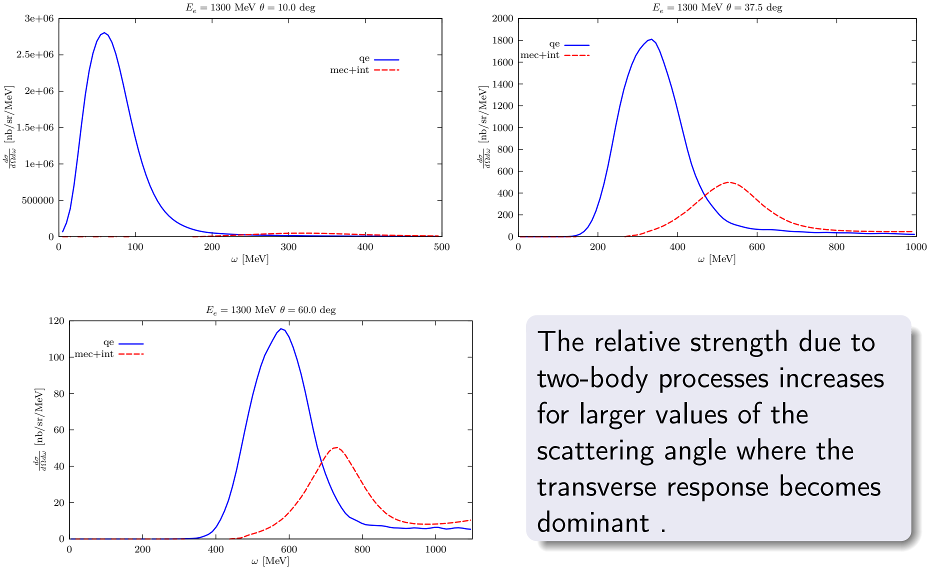

The relative strength due to two-body processes increases for larger values of the scattering angle where the transverse response becomes dominant .

Comparison of the results for the R_L of ^4He

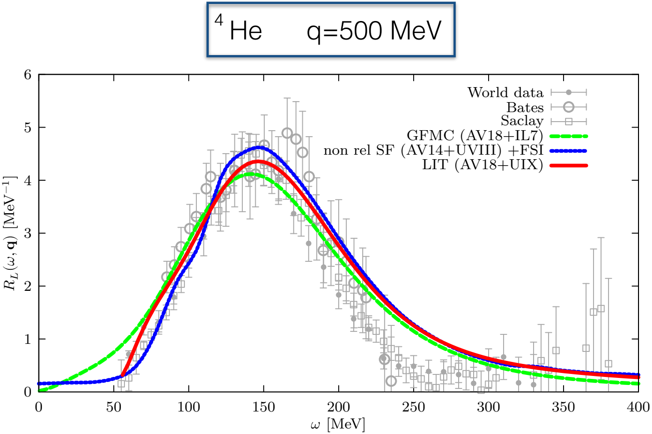

Good agreement...

The spread of the three curves is significantly smaller than the experimental errorbars

Different results obtained within GFMC and SF approach

^{12}C q=570 MeV

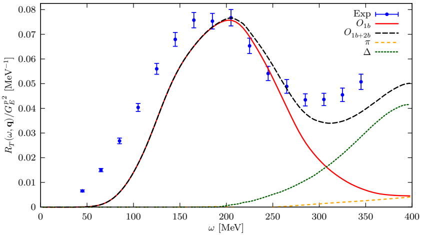

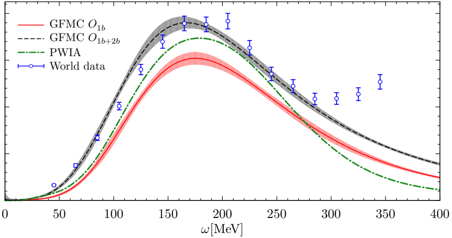

A. Lovato et al, arXiv:1605.00248

These differences should be ascribed to...

- Differences in the two-nucleon currents employed in the two cases
- The non relativistic nature of the GFMC calculations
- Interference between amplitudes involving the one- and two-body currents and 1p1h final states

Prospects . . .

- An accurate analysis of the role played by the interference between amplitudes involving the one- and two-body currents and 1p1h final states is currently being carried out.
- The implementation of our results in the determination of the nuclear response to electroweak probes will require the introduction of the one- and two-nucleon axial currents. This is crucial for a correct data analysis of neutrino oscillation experiments (T2K, MiniBooNE, MINERvA . . .)
- The technology based on Liquid Argon Time Projection Chambers (LAr-TPC), will be largely exploited by future experiments, such as DUNE, designed to carry out high-precision measurements of ν oscillations. This will require an extension of the spectral function formalism

Thank you!

backup slides

PHYSICAL REVIEW C VOLUME 58, NUMBER 1 JULY 1998

Exact ^{4}He spectral function in a semirealistic *NN* potential model

Victor D. Efros,[1] Winfried Leidemann,[2,3] and Giuseppina Orlandini[2,3]
[1]*Russian Research Centre "Kurchatov Institute," Kurchatov Square 1, 123182 Moscow, Russia*
[2]*Dipartimento di Fisica, Università di Trento, I-38050 Povo (Trento), Italy*
[3]*Istituto Nazionale di Fisica Nucleare, Gruppo collegato di Trento, Italy*
(Received 18 November 1997)

These results refer to a PWIA calculation $\longrightarrow$ FSI neglected

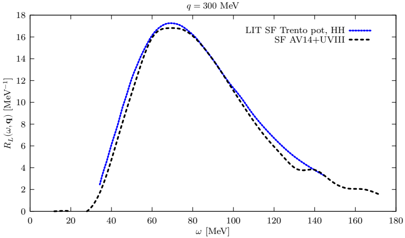

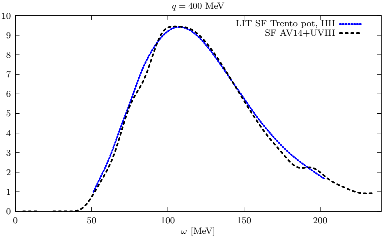

Final State Interaction in the SF formalism

Convolution approach

$$S(\mathbf{q},\omega) = \int d\omega' S_0(\mathbf{q},\omega) f_{\mathbf{q}}(\omega - \omega')$$

This expression can be obtained in a consistent fashion with a more fundamental approach

The Response of a system can be written in terms of the p-h propagator

$$S(\mathbf{q},\omega) = \frac{1}{\pi} Im\Pi(\mathbf{q},\omega) = \frac{1}{\pi} Im\Big[\langle 0|\rho^\dagger_q \frac{1}{H - E_0 - \omega - i\epsilon}\rho_q|0\rangle\Big]$$

In the limit of large momementum transfer, where the effect of long range correlations can be neglected,
$\Pi(\mathbf{q},\omega)$ can be written in terms of the p-h Green's functions.

Final State Interaction in the SF formalism

$$S(\mathbf{q},\omega) = \int d^3k dE P_h(\mathbf{k},E) P_p(\mathbf{k}+\mathbf{q},\omega - E)$$

Within the IA, where FSI are neglected

$$S_0(\mathbf{q},\omega) = \int d^3k dE P_h(\mathbf{k},E)\theta(|\mathbf{k}+\mathbf{q}| - k_F)\delta(\omega - E - E_{\mathbf{k}+\mathbf{q}})$$

Collecting together the above results, the p-SF can be written as

$$P_p(\mathbf{k}+\mathbf{q},\omega - E) = \theta(|\mathbf{k}+\mathbf{q}| - k_F)\int d\omega' f_{\mathbf{q}}(\omega - \omega')\delta(\omega' - E - E_{\mathbf{k}+\mathbf{q}})$$

and if we assume: $k + q \sim q \quad , \quad E_{\mathbf{k}+\mathbf{q}} \sim E_{\mathbf{q}}$

$$f_{\mathbf{q}}(\omega) = P_p(\mathbf{q},\omega + E_q)$$

The relevance of the interference term... $R_T(q, \omega)$

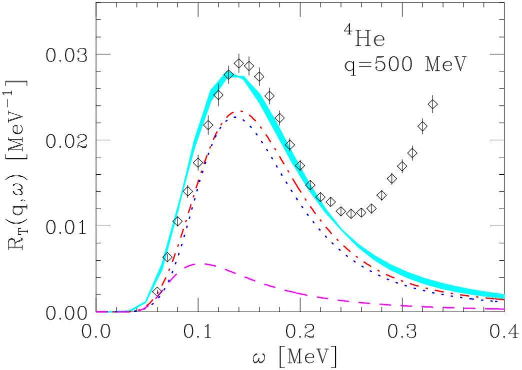

- Green's Function Monte Carlo calculation of the transverse electromagnetic response function of ^{4}He.
- MEC significantly enhance the transverse response function, not only in the dip region, but also in the quasielastic peak and threshold regions.

Inclusion of Final State Interaction contribution

- $f_{\mathbf{q}}(\omega - \omega' - U_V)$

- We consider $T_A = T_A(t_{kin})$ and $U_V = U_V(t_{kin})$ where

$$t_{kin} = \frac{E_k^2(1-\cos\theta)}{M + E_K(1-\cos\theta)}$$

- $F_{\mathbf{q}}(\omega)$ at $|\mathbf{q}| \sim 2$ GeV, including NN correlations

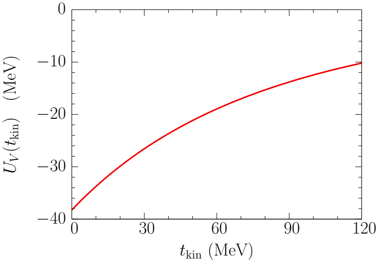

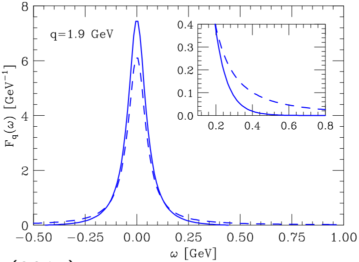

- A.Ankowski *et al.*, Phys. Rev. D 91, 033005 (2015)
- O. Benhar, Phys. Rev. C 87, 024606 (2013).

Extraction of the argon spectral function from $(e, e'p)$ data

- The spectral function will be obtained combining electron scattering data and the results of theoretical calculations, within the framework of the Local Density Approximation (LDA) $\Rightarrow$ **dedicated electron scattering experiment at JLab**

- Achieving this goal will require a careful analysis of the measured $(e, e'p)$ cross section as well as the extension of the existing studies of the nuclear matter spectral function to the case of a two-component system, needed to describe non isospin-symmetric matter.

The relevance of the interference term. . . Sum Rule

- Sum rule of the electromagnetic response in the T channel

$$S_T(\mathbf{q}) = \int d\omega S_T(\mathbf{q},\omega), \quad S_T(\mathbf{q},\omega) = S^{xx}(\mathbf{q},\omega) + S^{yy}(\mathbf{q},\omega) \ ,$$

where

- $S^{\alpha\beta} = \sum_N \langle 0|J_A^\alpha|N\rangle\langle N|J_A^\beta|0\rangle\delta(E_0+\omega-E_N)$

- Need for a consistent treatment of *both* correlations and MEC currents.

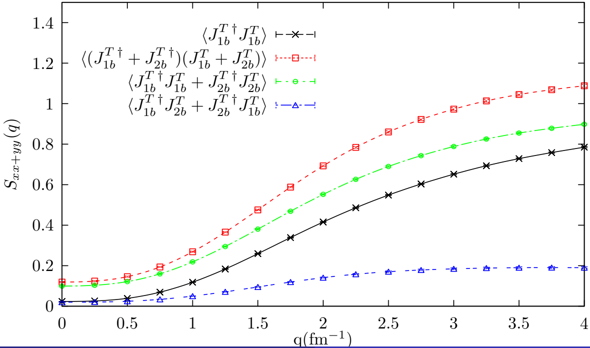

Two-body contribution within the SF anf FG formalism

The introduction of the two-nucleon current contributions in theoretical approaches based on the independent particle model (IPM) of nuclear structure, provides a quantitative wealth of the experimental data.

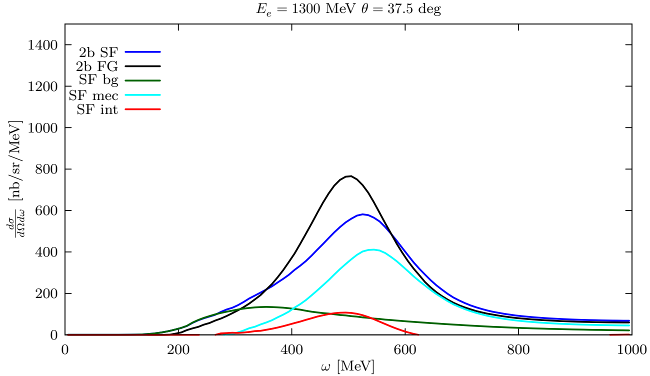

- The total two-body contribution obtained within the SF formalism do not differs too much from the FG result.

e^--^{12}C cross section within the SF and FG formalism

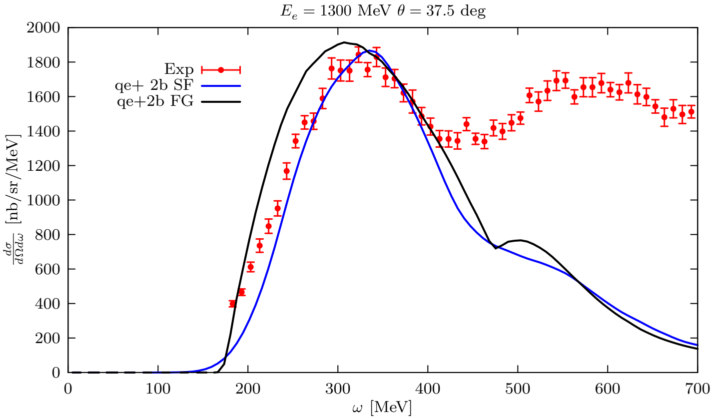

- While there are sizable differences both in the position and width of the QE peak, in the "dip" region the results obtained for the e^--^{12}C cross section within the SF and FG approaches do no differ significantly.

"Flux averaged" QE electron-Carbon cross section

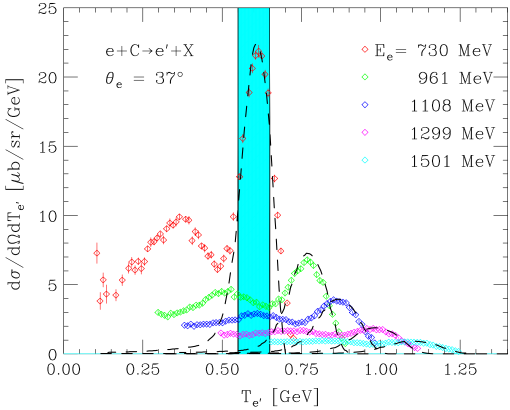

- Electron-Carbon scattering cross sections at $\theta_e = 37^\circ$ plotted as a function of $T_{e'}$.
- Reaction mechanisms other that single-nucleon knockout contribute to the "flux-averaged" cross section.

- development of models based on a new paradigm, in which all relevant reaction mechanisms are *consistently* taken into account within a unified description of nuclear dynamics.

The IA x-section

- The hadronic tensor can be written in the simple form

$$W_A^{\mu\nu} = \int d^3p dE\, P(\mathbf{p}, E)\, \frac{M}{E_p} \left[Z W_p^{\mu\nu} + (A - Z) W_n^{\mu\nu} \right] \ ,$$

- Elements entering the definition of the IA x-section
  - the tensor describing the interactions of the *i*-th nucleon in free space

$$W_\alpha^{\mu\nu} = \sum_X \langle -\mathbf{p}_R, N | {j^\mu}_\alpha^\dagger | X, \mathbf{p}_X \rangle \langle X, \mathbf{p}_X | j_\alpha^\nu | - \mathbf{p}_R, N \rangle \delta^{(4)}(\tilde{q} - p_R - p_X) \ .$$

$$\tilde{\omega} = E_X - \sqrt{\mathbf{p}^2 + M^2} = \omega + M - E - \sqrt{\mathbf{p}^2 + M^2}$$

  - The nucleon energy and momentum distribution, described by the hole spectral functions

Violation of current conservation

The replacement of ω with $\tilde{\omega}$ leads to a violation of the current conservation:

$$q_\mu w_N^{\mu\nu} = 0$$

Prescription proposed by *de Forest*:

$$\tilde{w}_N^{\mu\nu} = w_N^{\mu\nu}(\tilde{q})$$

$$\tilde{w}_N^{3\nu} = \frac{\omega}{|\mathbf{q}|} w_N^{0\nu}(\tilde{q})$$

The violation of gauge invariance only affects the longitudinal response. As a consequence, it is expected to become less and less important as the momentum transfer increases, electron scattering at large $|\mathbf{q}|$ being largely dominated by transverse contributions.

Local Density Approximation (LDA) P($\mathbf{k}$, E) for oxygen

$$P_{LDA}(\mathbf{p}, E) = P_{MF}(\mathbf{p}, E) + P_{\rm corr}(\mathbf{p}, E)$$

- $P_{MF}(\mathbf{p}, E) \rightarrow$ from $(e, e'p)$ data
- $P_{\rm corr}(\mathbf{p}, E) \rightarrow$ from uniform nuclear matter calculations at different densities:

$$P_{MF}(\mathbf{p}, E) = \sum_{n \in \{F\}} Z_n |\phi_n(\mathbf{p})|^2 F_n(E - E_n)$$

$$P_{\rm corr}(\mathbf{p}, E) = \int d^3 r \varrho_A(\mathbf{r}) P^{NM}_{\rm corr}(\mathbf{p}, E; \varrho = \varrho_A(\mathbf{r}))$$

Form factors

Hadronic monopole form factors

$$\begin{aligned} F_{\pi NN}(k^2) &= \frac{\Lambda_\pi^2 - m_\pi^2}{\Lambda_\pi^2 - k^2} \\ F_{\pi N\Delta}(k^2) &= \frac{\Lambda_{\pi N\Delta}^2}{\Lambda_{\pi N\Delta}^2 - k^2} \end{aligned} \tag{1}$$

and the EM ones

$$\begin{aligned} F_{\gamma NN}(q^2) &= \frac{1}{(1 - q^2/\Lambda_D^2)^2} \ , \\ F_{\gamma N\Delta}(q^2) &= F_{\gamma NN}(q^2)\Big(1 - \frac{q^2}{\Lambda_2^2}\Big)^{-1/2}\Big(1 - \frac{q^2}{\Lambda_3^2}\Big)^{-1/2} \end{aligned} \tag{2}$$

where $\Lambda_\pi = 1300$ MeV, $\Lambda_{\pi N\Delta} = 1150$ MeV, $\Lambda_D^2 = 0.71 \mathrm{GeV}^2$, $\Lambda_2 = M + M_\Delta$ and $\Lambda_3^2 = 3.5\ \mathrm{GeV}^2$.

Neutral weak current two-body contributions

The enhancement due to two- nucleon currents, at $q \simeq 1\ \mathrm{fm}^{-1}$, is about 50% relative to the one-body values.

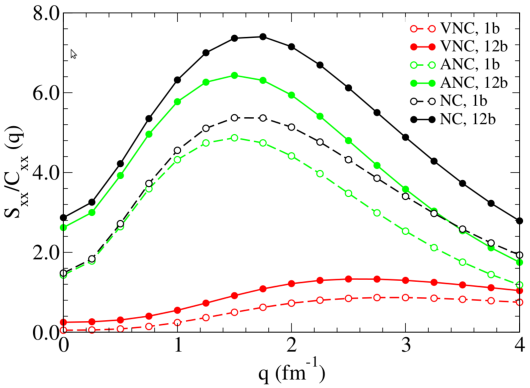

- A.Lovato *et al.*, Phys. Rev. Lett. 112, 182502 (2014)

- Low momentum transfer the dominant contribution is given by: $\langle i|j^\dagger_{2b} j_{2b}|i\rangle$
- At higher momentum transfer: $\langle i|j^\dagger_{2b} j_{1b}|i\rangle + \langle i|j^\dagger_{1b} j_{2b}|i\rangle$ plays a more important role.